The sea ice component of the coupled climate model HadGEM1

A. McLaren, H. Banks, C. Durman, J. Gregory, T. Johns, A. Keen, J. Ridley, M. Roberts (Hadley Centre, Met Office, UK)
W. Lipscomb (Los Alamos National Laboratory, New Mexico, USA)
S. Laxon (Centre for Polar Observation and Modelling, University College London, UK)
W. Connolley (British Antarctic Survey, Cambridge, UK)

SUMMARY

HadGEM1 is a new coupled atmosphere-ocean climate model developed at the Met Office's Hadley Centre, which contains a more sophisticated sea ice sub-model than that used in our previous climate model (HadCM3). A rapid increase in the variety, quality and quantity of observations in polar regions has led to a significant improvement in the understanding of sea-ice dynamic and thermodynamic processes and their representation in global climate models. We assess the simulation of sea ice in HadGEM1 against the latest available observations and against HadCM3. The evaluation is focused on the mean state of the key model variables of ice concentration, thickness and velocity. The model shows good agreement with the observations, except for ice speed, which is too fast. This could be either because the wind stress is too strong, or because the momentum coupling of the ice to the ocean is too weak. The variability of the ice forced by the North Atlantic Oscillation is also found to agree with observations.

1. MODEL AND EXPERIMENTAL DESIGN

The sea-ice model in HadGEM1 resolves the sub-gridscale ice thickness distribution by dividing the ice pack into five thickness categories and one open water category (leads). The ice velocities are calculated using the Elastic-Viscous-Plastic dynamics (EVP) of Hunke and Dukowicz (1997) and the amount of ice ridging is computed using the formulation of the CICE model (Hunke and Lipscomb, 2004). The ice growth/melt in each category is modelled using the zero-layer model of Semtner (1976) and the linear remapping scheme of Lipscomb (2001) is used to compute the thermodynamic transfer of ice between categories. For more details, see Hadley Centre Technical Note No. 55: http://www.metoffice.gov.uk/research/hadleycentre/pubs/HCTN/index.html.

Results from the HadGEM1 control simulation are examined which has fixed 1860 forcing levels for greenhouse gases, ozone, sulphur and other precursor emissions and land surface conditions. A 'spinup' integration of 85 years was first carried out, from which the control simulation was initialised. In this investigation we analyse data from the first 230 years of the control integration.

2. ICE AREA AND CONCENTRATION

The seasonal cycle of ice area for HadGEM1, HadISST (1979–2002) and HadCM3 is shown in **Figure 1**. HadGEM1's simulated ice area in both hemispheres is larger than observations. This is consistent with the model's pre-industrial forcing conditions.

Figure 2 shows that the ice undergoes rapid thermodynamic growth in the autumn, causing ice to be transferred through the thinnest categories. In the winter, ridging moves ice from the thinner to the thicker categories. The ice then melts back in the spring, with the thinner categories having larger seasonal cycles.

The spatial distribution of HadGEM1 March and September ice concentration (above 0.15) for the Northern and Southern Hemispheres is shown in **Figure 3**. The model's ice extent agrees well with HadISST (bold black line), apart from in the North Pacific in March where the ice is too extensive, consistent with the presence of a cold SST bias in this region.

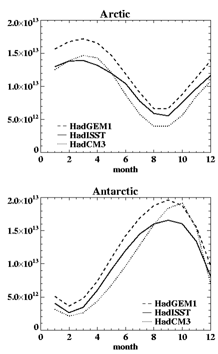

Figure 1: *Seasonal cycle of the ice area (m²) for HadGEM1, HadISST and HadCM3*

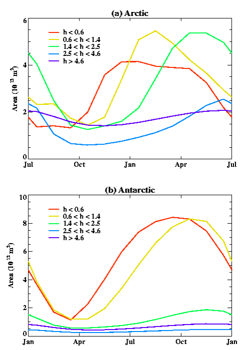

Figure 2: *Seasonal cycle of HadGEM1 ice area (m²) for the five thickness categories*

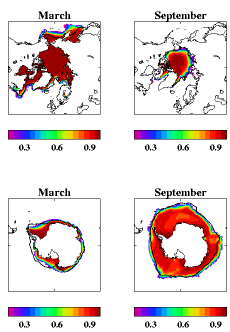

Figure 3: *HadGEM1 ice concentration. Thick lines show the extent (15%) for HadISST*

3. ICE THICKNESS

The model Arctic ice thickness is compared with the Radar Altimetry (RA) data of Laxon et al. (2003) in **Figure 4**. The ice in HadGEM1 is thicker in most of the Arctic Ocean, with differences of more than 0.5 m in the centre of the Beaufort Gyre. In contrast, the RA data is thicker in the eastern Beaufort Sea and the eastern Central Arctic, with values some 1 m thicker in the northern Barents Sea.

Figure 5 shows ice thickness for March and September for the Arctic and Antarctic respectively for HadGEM1 and HadCM3. The Arctic ice thickness maximum in HadCM3 is located in the Beaufort Gyre. In HadGEM1 however, the thickest ice is correctly banked up against the Greenland/Canadian coastline, in agreement with the RA and submarine data.

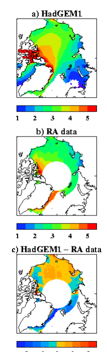

Figure 4: *Wintertime (Jan to Apr) mean ice thickness (m)* ***excluding open water and less than 0.5m thick***

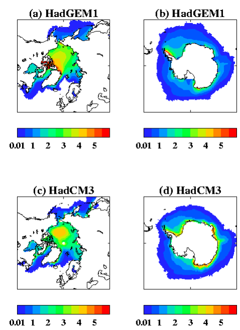

Figure 5: *Grid box mean ice thickness (m). (a) and (c): March, (b) and (d): September*

4. ICE VELOCITIES

Figure 6 shows ice velocities for the Arctic (March) and Antarctic (September) for HadGEM1 and observations (Fowler, 2003). In the central Arctic, the Beaufort Gyre and Transpolar Drift Stream features are well simulated by the model. The coherent southward movement of ice either side of Greenland is also captured by the model, but the speed of the ice is much too fast, partly driven by unrealistically high surface winds.

In the Antarctic, off-shore winds drive the ice away from the front of the major ice shelves as observed, allowing strong ice formation in the in-shore leads. However, the speed of the ice near the ice edge and close to the coastline is higher than suggested by the observations.

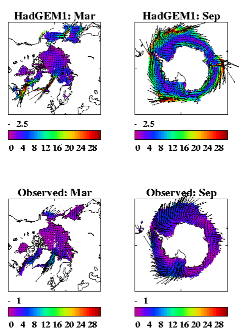

Figure 6: *Ice velocities (cm s⁻¹) for HadGEM1 and observations (Fowler, 2003)*

5. ICE RESPONSE TO NAO FORCING

HadGEM1 demonstrates a wintertime surface temperature response to high North Atlantic Oscillation (NAO) events (**Fig. 7**, top right, ˚C) which is consistent with observations (top left, ˚C). This temperature forcing contributes to a simulated ice concentration response (middle right) which is also generally consistent with observations (middle left).

However, the response of the wintertime ice thickness to high NAO events in the Beaufort Sea, for example, (bottom left: thickness anomalies (m)) appears to be a response to dynamic rather than thermodynamic forcing (bottom right: rate of change of ice thickness anomalies due to advective processes ($\times 10^{-8}$ m s^{-1})).

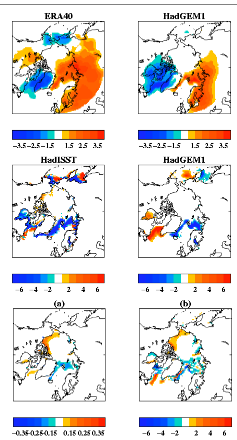

Figure 7: *NAO analysis*

REFERENCES

Fowler, C., 2003. Polar Pathfinder Daily 25 km EASE-Grid sea ice motion vectors. Boulder, CO, USA. NSIDC. Digital Media.
Hunke, E. and Dukowicz, J., 1997. An elastic-viscous-plastic model for sea ice dynamics. J. Phys. Oceanogr., 27, 1849–1867.
Hunke, E. and Lipscomb, W., 2004. CICE: the Los Alamos sea ice model documentation and software user's manual. Los Alamos National Laboratory.
Laxon, S. et al., 2003. High interannual variability of sea ice thickness in the Arctic region. Nature, 425, 947–950.
Lipscomb, W., 2001. Remapping the thickness distribution in sea ice models. J. Geophys. Res., 106, 13989–14000.
Semtner, A., 1976. A model for the thermodynamic growth of sea ice in numerical investigations of climate. J. Phys. Oceanogr., 6, 379–389.

ACKNOWLEDGEMENTS

This work was supported by the UK Government Meteorological Research Programme and the Climate Prediction Programme of the UK Department of the Environment, Food and Rural Affairs.

The EVP, ridging and linear remapping scheme code are based on the CICE model (Hinke and Lipscomb, 2004).

Met Office Hadley Centre FitzRoy Road Exeter Devon EX1 3PB United Kingdom
Tel: 01392 885680 Fax: 01392 885681
Email: ann.keen@metoffice.gov.uk